MATERIALS CHEMISTRY FRONTIERS

REVIEW

View Article Online
View Journal | View Issue

Cite this: *Mater. Chem. Front.*, 2021, **5**, 6413

Received 7th June 2021,
Accepted 6th July 2021

DOI: 10.1039/d1qm00834j

rsc.li/frontiers-materials

Nonlinear optics of graphdiyne

Chao Liu,[a] Xiao Han,[a] Rongchao Shi,[a] Siming Qi,[a] Songhua Chen,*[b] Liang Xu[c] and Jialiang Xu*[a]

Graphdiyne (GDY), as a rising star of all-carbon materials, features a high degree of π-conjugation, uniformly distributed pores, and an intrinsic natural bandgap. These characteristics guarantee a large optical refractive index, low saturation intensity, and broadband absorption, which promises a wide range of application prospects in the field of nonlinear optics (NLO). In recent years, research on GDY in the field of NLO has become increasingly prevalent. In this review, we discuss the research progress on GDY in the domain of NLO. The corresponding bottlenecks and challenges for the future development of GDY in NLO are discussed.

1. Introduction

In the past decades, all-carbon materials have been rapidly developed at the forefront of organic and inorganic chemistry as well as materials science. Carbon allotropes such as natural graphite (sp^2),[1] low-dimensional fullerenes (sp^2),[2–4] carbon nanotubes (sp^2),[5] graphene (sp^2),[6,7] and diamond (sp^3)[8] have received extensive research attention for their special structures and optoelectric properties.[1,9,10] The discovery of carbon-rich materials and their excellent optoelectronic properties has greatly accelerated the development of various sciences in the world today. It is well known that sp hybrid carbon atoms have linear structures, a high degree of π-conjugation, and no *cis*/*trans* isomerization characteristics. The outstanding physical structure of carbynes gives them unusual electrical, optical and catalytic properties.[11] Moreover, the combination of carbon allotropes and sp hybrid carbon–carbon triple bonds, such as the combination of sp and sp^2, and the combination of sp and sp^3, have led to many different and interesting properties that have stimulated many theoretical and experimental studies.[12,13]

The first theoretical studies on graphyne were presented in 1987 by Baughman and his colleagues who estimated its structure and electronic properties.[14,15] Different from other two-dimensional carbon materials, Graphdiyne (GDY) is a new type of carbon allotrope, composed of sp and sp^2 hybridized carbon atoms. The special extended connection of hybridized carbon atoms renders GDY a two-dimensional planar structure.[16–19] GDYs express uniformly distributed pores, a high degree of π-conjugation, natural bandgap, broadband absorption, and tunable electronic properties.[20–23] Moreover, the carbon–carbon triple bonds make it feasible to introduce adsorbed atoms (*e.g.*, fluorine, hydrogen, or oxygen) to obtain various GDY derivatives. In recent years, GDY and GDY derivatives have been widely employed for broad applications in catalysis,[24–28] energy storage,[29–34] biomedicine,[21,35–37] solar cells,[38–40] nonlinear photonics,[41] random lasers,[42] and other frontier fields for their unique structures as well as physical and chemical properties. Comprehensive experimental studies on NLO properties of two-dimensional materials have been carried out since the advent of graphene.[43,44] As a two-dimensional isomer of graphene, GDY has also demonstrated promising applications in nonlinear optics.[45–47]

[a] *School of Materials Science and Engineering, National Institute for Advanced Materials, Nankai University, Tianjin 300350, P. R. China. E-mail: jialiang.xu@nankai.edu.cn*
[b] *College of Chemistry and Material Science, Longyan University, Longyan 364012, Fujian, P. R. China. E-mail: songhua@iccas.ac.cn*
[c] *Department of Chemistry and Key Laboratory for Preparation and Application of Ordered Structural Materials of Guangdong Province, Shantou University, Shantou, Guangdong 515063, P. R. China*

Jialiang Xu

Jialiang Xu is a Professor of Materials Chemistry at Nankai University. He obtained his PhD from the Institute of Chemistry, Chinese Academy of Sciences (ICCAS) in 2010 under the supervision of Prof. Yuliang Li, and then worked as a Marie-Curie fellow at Radboud University, Nijmegen, hosted by Prof. Alan Rowan and Prof. Theo Rasing. In 2013, he was awarded the NWO-VENI grant, with which he developed his research profile at the interface between chemistry and physics to study the coupling between light and (supra) molecular systems. He joined Tianjin University in 2015 and relocated to Nankai University in 2018.

The high-quality, large-scale synthesis of single-layer GDY is a necessary condition for studying its intrinsic properties. In 2010, Li *et al.* prepared a large area of GDY film on a copper surface through the cross-coupling reaction of hexaacetylenebenzene, and showcased its excellent semiconductor properties.[19] In this case, copper foil not only serves as the catalyst in the cross-coupling reaction but also offers the substrate for the growth of GDY film.[48] Since then, chemists have carried out comprehensive experimental studies on the controllable synthesis of GDY. In 2012, Li *et al.* employed the vapour–liquid–solid (VLS) growth process to successfully prepare high-quality GDY nanowires with surface defects and semiconductor properties.[49] In 2015, Liu *et al.* successfully synthesized uniform GDY nanowalls on the surface of copper substrates by the Glaser–Hay reaction.[50] Subsequently, 2D GDY nanowalls,[26] nanosheets,[51–53] and 3D GDY frameworks[53,54] have been synthesized in succession. In 2017, Matsuoka *et al.* used the liquid–liquid interface method to obtain multi-layer GDY *via* continuous alkyne–alkyne conjugation reactions at the interface.[51] In 2019, Zhang *et al.* synthesized ultra-thin GDY with a smooth, continuous surface and good crystallinity using graphene as a template.[55] The synthesis of ultra-thin GDY undoubtedly provides possibilities for studying the essential characteristics of GDY, which also accelerates the application and development of GDY in various fields. Recently, Zhao *et al.* successfully prepared highly ordered graphtetrayne (GTTY) crystals with precisely controlled and well-defined chemical structures on copper surfaces.[56]

The successful synthesis of GDY has undoubtedly accelerated the exploration and application of its functionalities.[57–59] NLO of GDY has also attracted broad interest in this context. In this review, we focus on the research progress of GDY in the field of nonlinear optics. We will present the electronic structures and optical properties of GDY both theoretically and experimentally to identify the key factors for the excellent performance of GDY in NLO. Finally, we will discuss some of the problems and challenges GDY will face in its future development in the field of NLO.

2. Linear optical properties of GDY

2.1 Electronic structures and properties

The electronic structures and properties of GDY have been explored to intensively unravel its linear and nonlinear optical properties. Notably, GDY has two self-doped, non-equivalently distorted Dirac cones.[60,61] First-principles calculations have shown that the GDY family generally has an intrinsic bandgap of 0.44 to 1.22 eV, which is very different from the zero bandgap of graphene.[18,62–64] It is known that the presence of direct bandgaps may facilitate the applications of GDY in optoelectronic devices. Meanwhile, the electronic properties can be tuned by varying the number of layers of GDY.[65] Luo *et al.* reported the electronic structure of GDY based on first-principles calculations.[62] The geometry of the GDY, the unit cell, the coordinate base points, and the first Brillouin band are shown (Fig. 1a). By comparing the band structure and state density of GDY calculated at the LDA level and GW level, considering the quasi-particle effect, the results show a bandgap of 0.44 eV at the

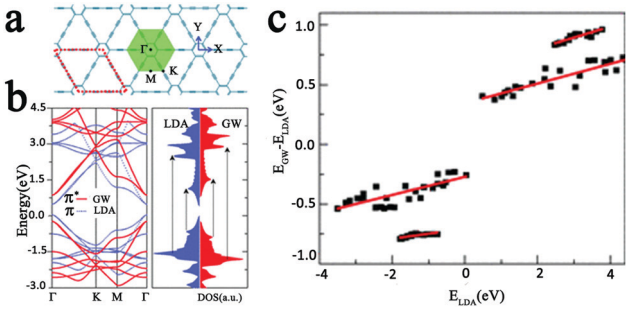

Fig. 1 Electronic properties of GDY. (a) Geometrical structure, unit cell (red dashed diamond), coordinate bases, and first Brillouin zone (green hexagon) of GDY. (b) Band structures and density of states (DOS) of GDY at the LDA and GW levels. (c) Quasiparticle correction as a function of the LDA energy in GDY. The linear fit of the data is plotted in red lines. Reprinted with permission from ref. 62, Copyright 2011, American Physical Society.

LDA level. However, there is a clear increase to 1.10 eV at the GW level (Fig. 1b). Such a 1.5 times quasiparticle correction is the consequence of the enhanced coulombic interaction in reduced dimensionality. It is worth mentioning that the corrections to the conduction and valence bands by quasiparticles can be divided into two categories based on the magnitude of the corrections (Fig. 1c). The electronic structure of GDY varies with its structural stacking modes.[66] Lu and co-workers have systematically studied the structural and electronic properties of the bilayer and trilayer GDY.[65] The results show that the most stable bilayers and trilayers of GDY all have their hexagonal carbon rings stacked in a Bernal mode, and the possible configurations of bi- and trilayer GDY systems are shown in Fig. 2a and b. The direct bandgaps for the most stable and second most stable stacking arrangements of double-layered GDY are 0.35 eV and 0.14 eV, respectively (Fig. 2c), and the bandgap for the three-layer GDY stable stacking style is 0.18 to 0.33 eV (Fig. 2d). Interestingly, GDY has a theoretical carrier mobility of up to 2×10^5 cm^2 (V^{-1} s^{-1}) at room temperature, which is higher than that of graphene two-dimensional material.[64]

Electron modulation properties of 2D materials are crucial for their applications. Alterations in edge morphology, strain and ribbon width, and doping with heteroatoms can effectively tune their electronic structures.[61,65,67–71] For instance, by utilizing the first-principles calculations combined with the tight-binding approximation, the strain-induced semiconductor–semimetal transition in GDY was discovered. The bandgap of GDY increased from 0.47 eV to 1.39 eV with enhancing the biaxial tensile strain, while the bandgap decreased from 0.47 eV to nearly zero with weakening the uniaxial tensile strain (Fig. 3a–d). The broken geometrical symmetry led to an increase in energy band degeneracy.

Chemical doping is another effective means of modulating the electronic structures of GDY.[72,73] Band structures of N-, P- and As-doped GDY with hexagonal and rectangular atomic lattices as shown in Fig. 3e demonstrated their bandgaps of 1.27, 1.90, 1.55, 2.23, 0.76, and 0.75 eV, respectively. Significantly, the optimum bandgap for photovoltaic devices should be in the range between 1.1 and 1.4 eV.[74,75] Therefore, doped

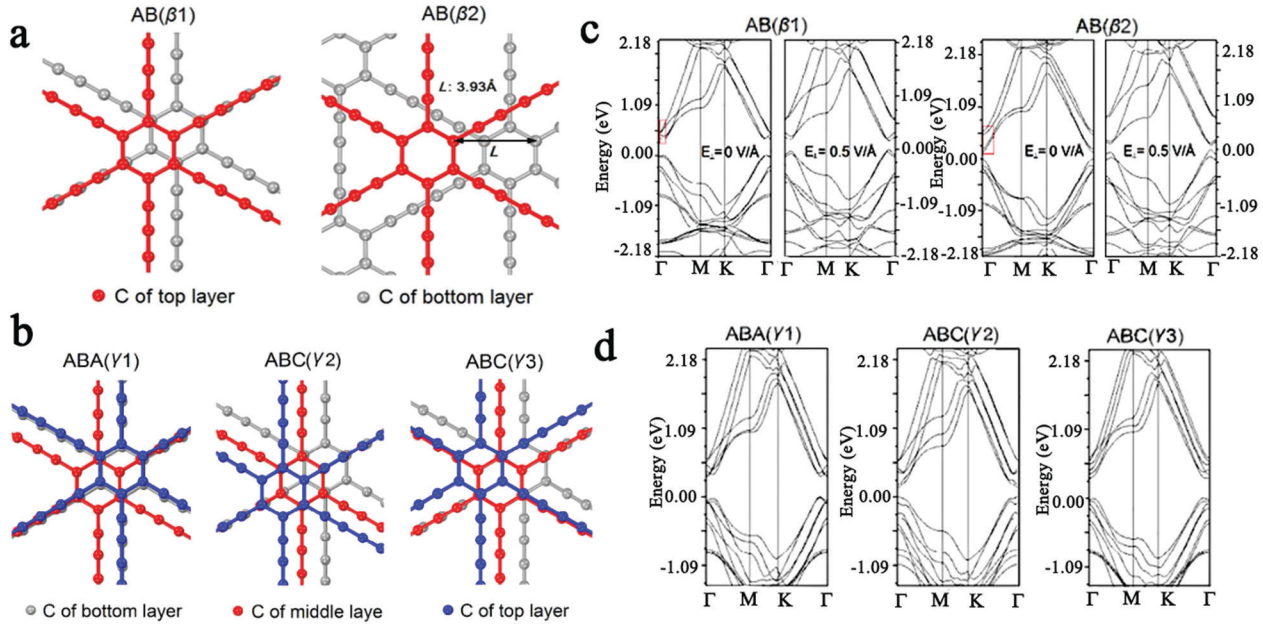

Fig. 2 Electronic properties of the bilayer and trilayer GDY. (a) Optimized configurations of bilayer GDY, referred to as AB(β1) and AB(β2), respectively. (b) Three possible configurations of the trilayer GDY from the top view: ABA(γ1), ABC(γ2), and ABC(γ3) configurations, respectively. (c) Band structures of bilayer GDY. The two red boxes indicate the two groups of bilayer GDY bands whose energy difference stems from the monolayer LUMO and LUMO+1 interaction. (d) Band structure of trilayer GDY configurations of the ABA(γ1), ABC(γ2) and ABC(γ3), respectively. Reprinted with permission from ref. 65, Copyright 2012, The Royal Society of Chemistry.

GDY nanosheets are deemed to be ideal candidates for nano photovoltaic devices. The superiority of the electronic properties and flexible electronic configurations from GDY offer the potential to manufacture nanoscale semiconductor or optoelectronic materials in compact devices.

2.2 Optical properties

Light absorption is one of the most fundamental optical properties of two-dimensional materials. Since GDY is one the ideal candidates for optoelectronic materials, it is fundamental to have an understanding of its optical properties. The absorption spectrum of GDY was reported theoretically and experimentally by Luo *et al.*[62,68] The absorbance of GDY was measured in the NIR to UV region (blue line in Fig. 4a). After subtracting the background, the absorbance of the GDY films in the NIR to UV range is shown in Fig. 4b and then compared with theoretical results at the level of the stochastic phase approximation (GW + RPA) and the Bethe–Salpeter equation (BSE). The calculations show that the BSE levels give a result that best matches the experiment, and the three experimental absorption peaks of 0.56, 0.89, and 1.79 eV correspond to the BSE excitation peaks of 0.75, 1.00, and 1.82 eV, respectively. The first peak is from the transition around the bandgap, while the others are from around the van Hove singularities. Such a discrepancy is not surprising because the experimental samples are GDY films with interlayer van der Waals (vdW) interactions, which are known to reduce Coulomb interactions as the dimensionality increases, thus affecting the position of the exciton peaks. Graphyne and GDY have been investigated using density functional theory (DFT) and time-dependent density functional theory (TDDFT).[76] The graphyne absorption range (1.59–3.59 eV) was found to be wider than that of GDY (1.91–2.49 eV). Experimental results also showed that although graphyne and graphdiyne are both direct bandgap semiconductor materials, there are significant differences in their energy band structures.

Luo *et al.* investigated the optical properties of monolayer GDY and four different stacking systems using DFT plus vdW density functions.[68] Several stacking geometries of GDY are shown in Fig. 5a–c. The spectrum in the *Z* direction is omitted in this experiment because local field effects strongly suppress light absorption in the energy range of interest. The measured spectra display three main peaks located below 1 eV, around 1.7 eV, and around 4.02 eV, respectively (Fig. 5d–f). For the AA stacking, the spectra along the *X* and *Y* polarization directions are identical, with the lowest and most intense peak is located at 0.11 eV. The lowest peak of the AB-1 stacking is located at around 0.15 eV in both directions, but the intensity in the *Y* direction is ~40% stronger than that in the *X*-direction. In contrast, the spectral features of the AB-2 stack are very similar to those of the monolayer spectrum, except for a slight difference of around 0.7 eV as a result of a small degeneracy boost in the band structure. Finally, the spectrum of the AB-3 stack is characterized by two peaks in the *X*-direction, one at 0.28 eV and the other at 0.49 eV. Only a single peak is at 0.67 eV in the *Y*-direction. Compared to the spectra of monolayers of GDY, the peaks below 1 eV are generally redshifted in all the bulk structures due to the reduced or closed bandgap in the bulk structures. The system found the AA conformation to be the least stable structure after vdW correction, followed by the AB-1 conformation, with the AB-2 and AB-3 stacks being the two most stable structures.

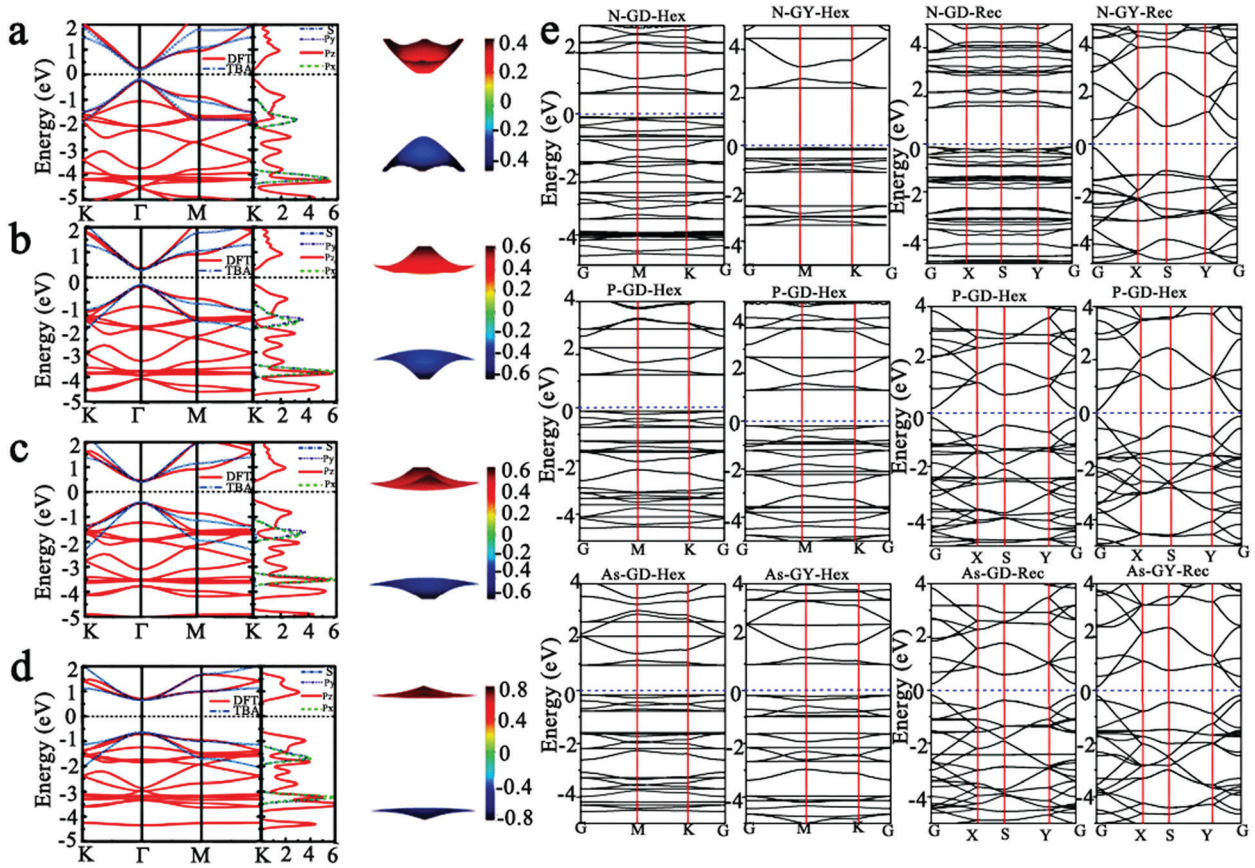

Fig. 3 Electrical properties of structurally modified and chemically doped GDY. The band structures calculated by density functional theory (DFT) and the tight-binding approximation (TBA), the partial density of states (PDOS) and the three-dimensional energy bands at the Γ point for GDY (a) without a strain, and under a symmetrical biaxial tensile strain of (b) 5%, (c) 9%, and (d) 15%, respectively. Reprinted with permission from ref. 61, Copyright 2013, The Royal Society of Chemistry. (e) Band structures of single-layered N-, P- and As-GDY/graphyne monolayers with hexagonal and rectangular atomic lattices predicted by the PBE functional. Reprinted with permission from ref. 72, Copyright 2019, The Royal Society of Chemistry.

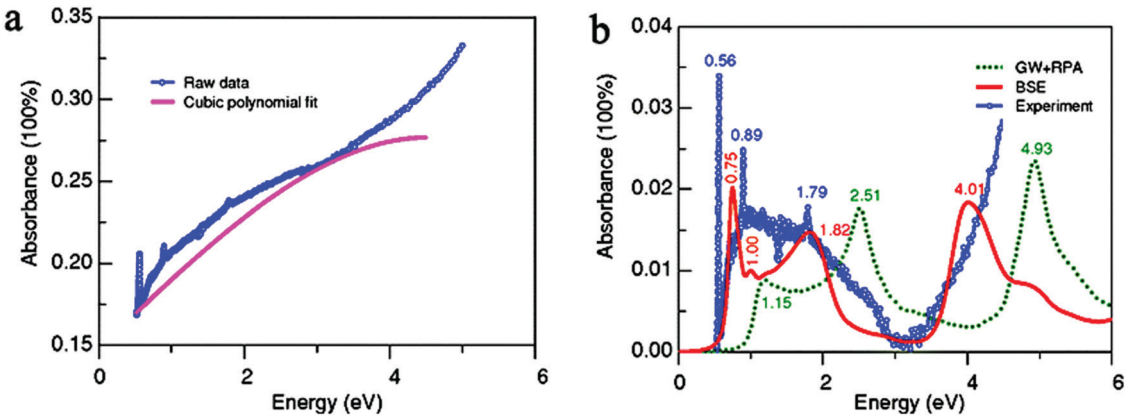

Fig. 4 Optical absorption properties of GDY. (a) Raw experimental absorbance (blue circle) of GDY film and cubic polynomial fit (pink solid line) for its background. (b) Experimental absorbance (blue circle) of GDY film and theoretical absorbance at the GW + RPA (green dotted line) and BSE (red solid line) levels of GDY. Reprinted with permission from ref. 62, Copyright 2011, American Physical Society.

The above analysis also proves that chemical doping can effectively change the electronic structure of GDY, so its optical properties will be changed accordingly.[69,70] Both chemical and functionalized modifications can effectively modulate the optical properties of GDY.[71,77] Azin Shahsavar *et al.* systematically studied the electronic structure and optical properties of modified graphene/GDY using first-principles DFT calculation methods. Theoretical calculation results showed that in the case of –O, –CO and –COH functional group modification, the charge transfer between the edge oxygen group and the carbon surface will cause

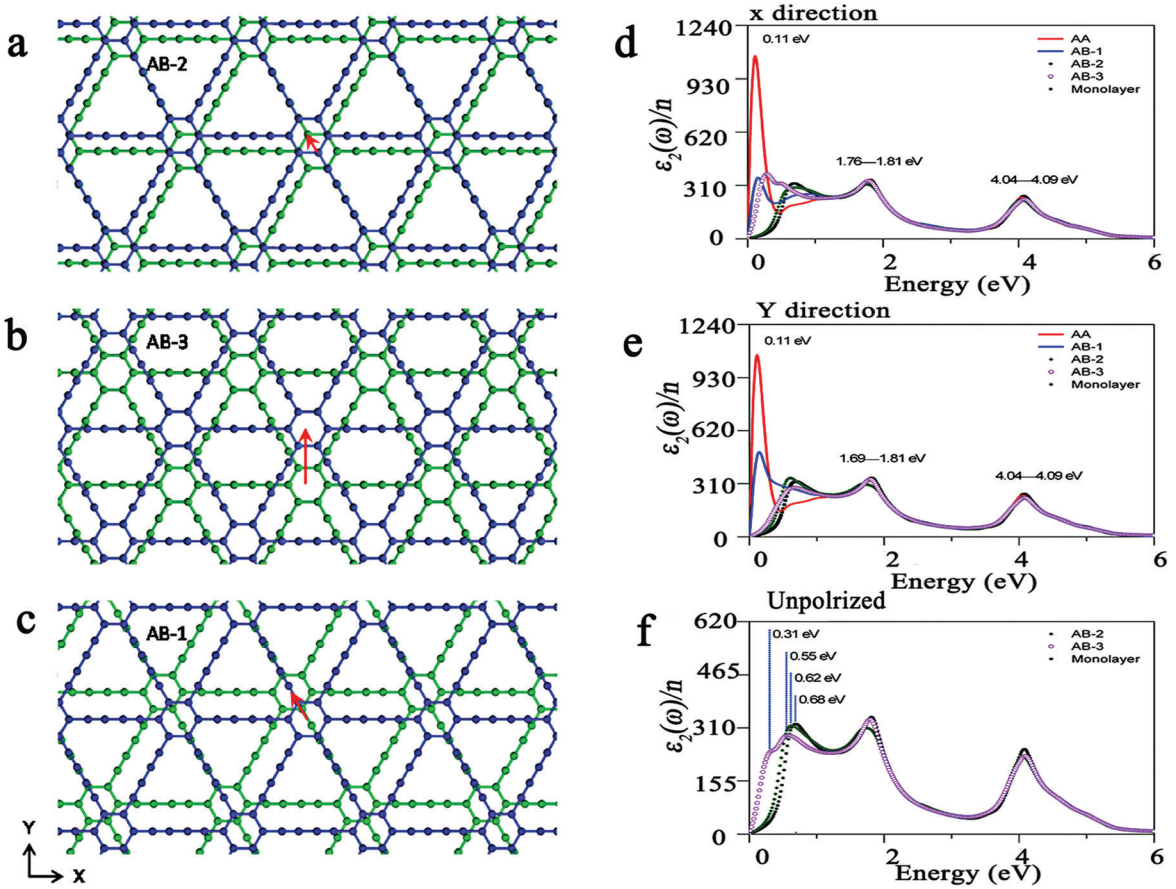

Fig. 5 Optical absorption of GDY with different stacked structures. Geometrical structures of the (a) AB-2, (b) AB-3, and (c) AB-1 stacked bulk GDY. The red arrows indicate the relative in-plane shifts of the two layers in a cell. Polarized optical absorption spectra of the AA, AB-1, AB-2, AB-3 stackings along the (d) *X*-, and (e) *Y*-directions. (f) Unpolarized optical absorption spectra of the AB-2 and AB-3 stackings. Reprinted with permission from ref. 68, Copyright 2013, American Chemical Society.

the DOS near the Fermi level to change drastically (Fig. 6a–c). It is worth noting that the introduction of oxygen-containing functional groups will cause electron transfer in the system, and then form p/n-type semiconductor materials, enriching the electrical properties of graphene/GDY. For the original graphyne and GDY nanosheets, the absorption starts from the UV region to the visible region. In the follow-up work, a wider spectral range from UV to NIR was observed after functionalization with –CO or –COOH groups. In general, the electronic energy spectrum of GY/GDY is redshifted due to functionalization with –CO and –COOH groups.[78] The degree of redshift is aggravated with the number of functional groups and the absorption intensity increases in the same way. This undoubtedly widens the range of applications for GDY in the field of optoelectronic devices.

3. Nonlinear optics of GDY

3.1 Second-order NLO of GDY

NLO studies the nonlinear interaction of matter with the electric field of intense light.[79,80] In 1961, the second harmonic generation (SHG) was first discovered by Franken *et al.*[81] This signified the beginning of the field of NLO. Since then, NLO has attracted widespread attention and has played an increasingly important role in the fields of optical information technology, lasers, and materials science.[82–86] Since the first NLO phenomenon was identified, SHG has been the most developed NLO effect in the field of laser technology. It is a typical second-order NLO phenomenon and can be described quantitatively in terms of the second-order NLO magnetisation.[87,88] SHG is a frequency doubling process, *i.e.*, two incident photons combine to produce a photon with doubled frequency and energy.[89] It is well known that SHG active material is characterized by the non-centrosymmetric (NCS) structure.[88–91] However, due to the limitations of the two-dimensional planar structure of GDY, the study of its second-order NLO is still at the stage of theoretical exploration.

Based on DFT, Li *et al.* reported that the adsorption of a single alkali metal (AM = Li, Na, K) on the surface of GDY NLO properties.[73,92] All alkali metals can interact and stabilize the intramolecular electron donor–acceptor process with the large triangular holes in the widely delocalized π-conjugated GDY through van der Waals interactions. According to calculations, the first hyperpolarizability (β_0) values of free graphene, graphyne, and GDY were expected to be less than 0.20 a.u. Nevertheless, after

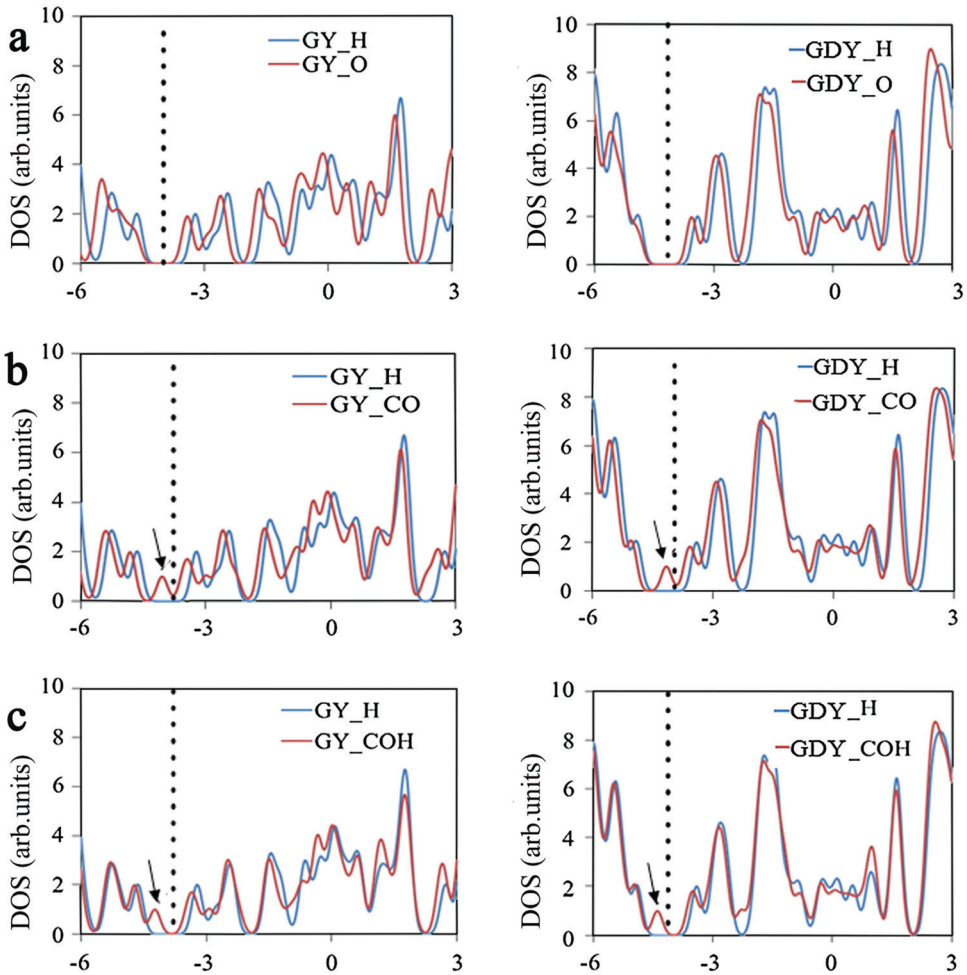

Fig. 6 Density of states (DOS) for the edge oxidized graphene (GY) (left) and GDY (right) functionalized by –O, –CO, and –COH functional groups. The dashed line shows the Fermi energy of the bare carbon surface and the arrows indicate the change in the state's location after functionalization. Reprinted with permission from ref. 71, Copyright 2016, Elsevier.

doping with alkali metals, the β_0 values of these complexes increased (Fig. 7a), which can be attributed to the gradual decrease in the electronegativity of the alkali metals from Li to K. On the other hand, this results from the valence electrons of the alkali metal atoms being readily transferred to the GDY group when they interact with GDY. It manifested that the main electronic leap in the key excited state of AM@GDY is from the HOMO−2 orbital to the LUMO transition (Fig. 7b). The experiment also analyzed the frequency dependence of the electro-optic (EO) Pockels effect and SHG and indicated that the SHG resonance enhancement occurred at ω = 0.10 a.u. (Fig. 7c). This study not only highlights the importance of single alkali metal adsorption on the GDY surface in improving its NLO performance but also reveals that AM@GDY complexes are promising as crucial materials for the next generation of GDY-based optoelectronics applications. Adding extra electrons to the system will directly affect the NLO properties of the material, increasing its first hyperpolarizability, which provides guidance for the design of new NLO materials.[92–97] The adsorption of alkali metal atoms on different nanostructures is an effective way to obtain excess electrons in the system.[98,99] Mahmood *et al.* adopted DFT calculations to design a series of new superalkali-doped GDY complexes with electron donor and acceptor frameworks (M_2X@GDY, M = Li, Na, K, and X = F, Cl, Br).[100] DFT results show that the doping of superalkali on GDY leads to the reduction of the HOMO–LUMO gap, thereby enhancing its electrical conductivity. The polarizability and first hyperpolarizability of GDY were also significantly improved, with the highest value reaching 7.7×10^4 a.u. (Fig. 8a and b). It ought to be stated that the value of the first hyperpolarizability is mainly influenced by the interaction distance between the dopant and the complexing agent, and the magnitude of the ionization energy.[101,102] When the size of the alkali metal atoms increases, the ionization potential decreases and excess electrons are generated, which leads to an increase in the hyperpolarizability. With the increase of the atomic radius, the ionization energy gradually decreases, the value of β_0 increases from Li_2F@GDY to Na_2F@GDY and from Li_2Br@GDY to Na_2Br@GDY, while the value of β_0 increases from Na_2F@GDY to K_2F@GDY and from Na_2Br@GDY to K_2Br@GDY. The gradual decrease is due to the larger interaction distance. In the M_2Cl@GDY system, the transition energy gradually decreases, causing the β_0 value to show an increasing trend. In a recent study, Mahmood *et al.*

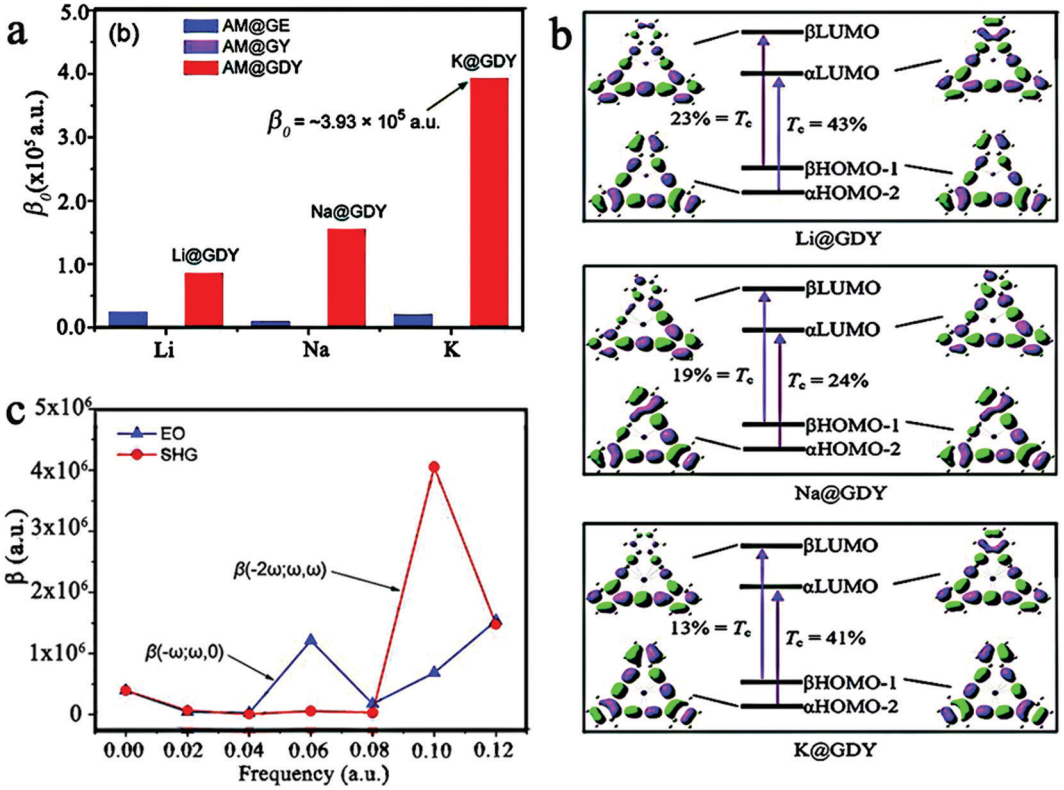

Fig. 7 (a) Static first hyperpolarizability (β_0) of AM@GE, AM@GY, and AM@GDY (AM = Li, Na, K) complexes determined at the CAM-B3LYP/6-311++G(2d,2p) level. (b) Main electronic transitions in crucial excited states (Tc) of the Li@GDY, Na@GDY, and K@GDY complexes determined using the CAM-B3LYP method. (c) Frequency dependence of the two different first hyperpolarizability (β) processes of K@GDY. EO: electro-optical Pockels effect with $\beta(-\omega; \omega, 0)$; SHG: second-harmonic generation with $\beta(-2\omega; \omega, \omega)$, determined at the CAM-B3LYP/6-311++G(2d,2p) level of theory. Reprinted with permission from ref. 73, Copyright 2019, The Royal Society of Chemistry.

studied the NLO properties of superalkali-doped graphdiyne complexes (Na_2Y@GDY, Y = SH, OCH_3, SCH_3, CN and N_3) and M_3O, M_3S (M = Li, Na, and K)-doped GDY complexes.[103,104] In both experimental schemes, superalkali doping is used to introduce excess electrons into the system and generate new HOMO orbitals to reduce the HOMO–LUMO gap. The analysis showed that in all superalkaline-doped GDY complexes, the charge was transferred from the superalkaline to GDY. At the same time, the superalkali doping greatly enhanced the first hyperpolarizability β_0 of GDY. DFT calculation results showed that the highest β_0 (6.17×10^4 a.u.) was observed in the Na_2OCH_3@GDY complex. In Na_3S@GDY, the largest first hyperpolarizability was observed to be 1.36×10^5 a.u. Thus, the two-level model can well explain why Na_2OCH_3@GDY and Na_3S@GDY exhibited a larger NLO response (Fig. 8c). Note that the transition energy is a key factor in enhancing the first hyperpolarizability of these complexes. It should also be noted that two-dimensional layered materials with multiplicative effects generally appear only in structures with inverse symmetry breaking, and in recent years SHG responses have been found in some layered two-dimensional materials, such as graphene-like materials,[105–107] transition metal sulfides (TMDCs),[108–110] *etc.* Taking h-BN and $PdSe_2$ as examples, the SHG signal of h-BN appears in odd layers and disappears in even layers. Such a high contrast is due to the presence of the second harmonic polarization in the unimolecular layer, which is absent in the bimolecular layer due to stacking.[106] For $PdSe_2$, on the contrary, the SHG signal appears in the even layer, while the signal in the odd layer is negligible because the odd layer crystallizes in the space group with inversion symmetry, while the even layer crystallizes in the space group with broken inversion symmetry.[110] The intrinsic SHG signal of the non-centrosymmetric structure is also affected by the applied electric field and doping.

3.2 Third-order NLO of GDY

Third-order NLO does not require an NCS configuration.[111,112] Therefore, a wider variety of two-dimensional materials will be available and effective in third-order NLO. It has been confirmed that GDY has ideal NLO characteristics in the visible wavelength band, which provides a strong guarantee for its application in the field of NLO. Wu *et al.* skilfully applied this new type of material to nonlinear photonic diodes and introduced another antisaturable absorption material (SnS_2) to combine these two 2D materials in the form of liquid or thin films. The results show that the nonlinear photonic diode is capable of non-reciprocal propagation of light.[41] When a laser beam with a relatively high intensity passes through the forward direction (GDY/SnS_2), the diffraction ring will be excited due to the strong NLO response of the GDY caused by the Kerr effect. However, when a laser beam of the same intensity passes in the opposite direction (SnS_2/GDY), no diffraction ring can be produced.

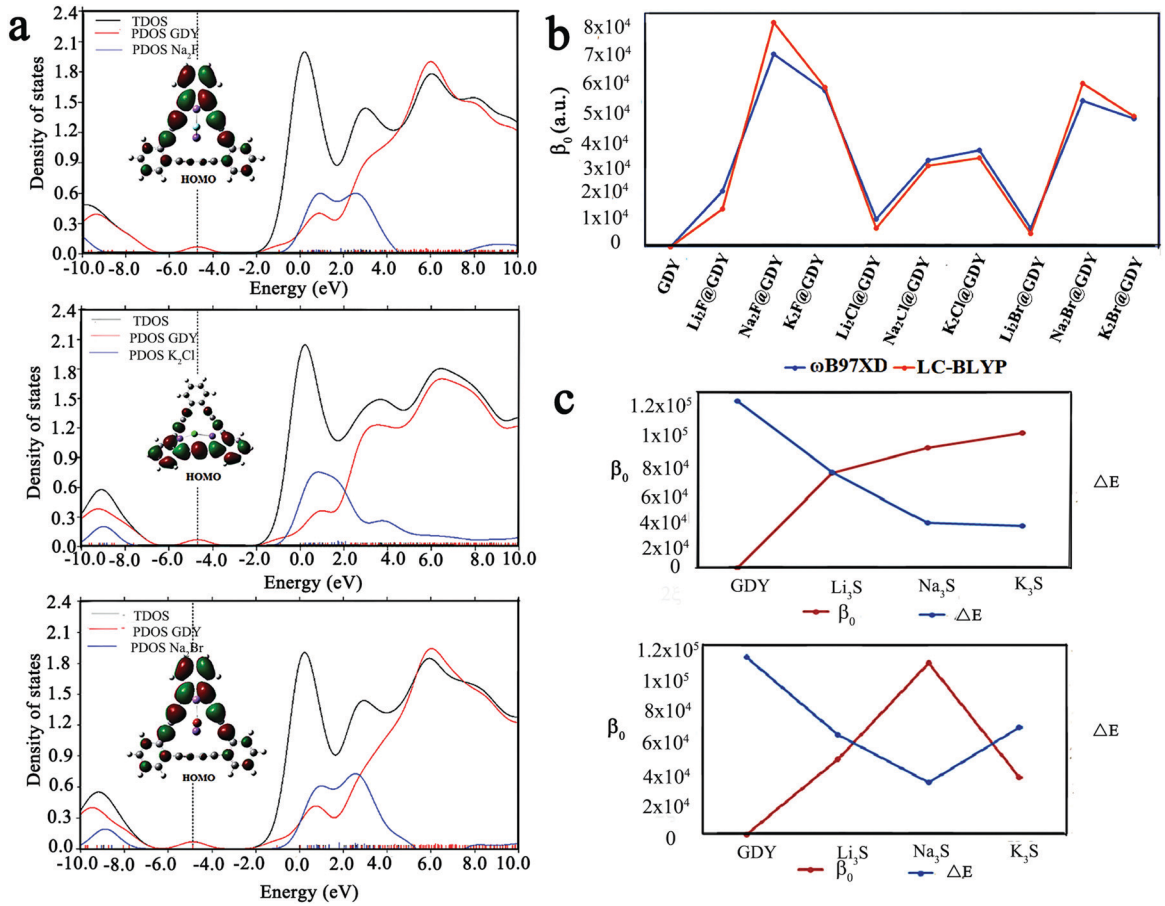

Fig. 8 (a) TDOS and PDOS spectra of superalkali-doped GDY complexes (Na_2F@GDY, K_2Cl@GDY and Na_2Br@GDY). (b) Comparison of the first hyperpolarizability between long-range separated functionals. Reprinted with permission from ref. 100, Copyright 2019, Elsevier. (c) Comparison of the calculated first hyperpolarizability (β_0) and ΔE of both M_3O@GDY and M_3S@GDY complexes. Reprinted with permission from ref. 104, Copyright 2020, Elsevier.

The reason is that SnS_2 has strong linear absorption and severely reduces the intensity of incident light (Fig. 9a–f). In this way, the strong nonlinear effect exhibited by GDY not only provides the possibility for its application in photonic diodes but also shows an ideal application prospect in all-off modulation and switching.

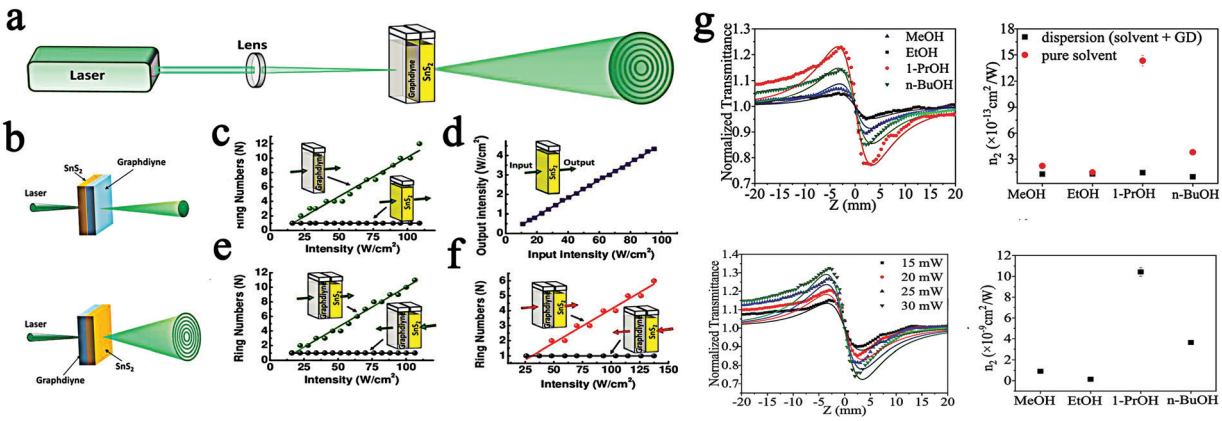

Fig. 9 (a) The experimental setup for the proposed GDY/SnS_2 based nonlinear photonic diode. (b) The phenomenon of the nonreciprocal light propagation observed from the proposed nonlinear photonic diode. (c) The number of diffraction rings excited from the independent GDY dispersions and SnS_2 dispersions at λ = 532 nm. (d) The input and output intensity of the 532 nm laser beam before and after it passes through the SnS_2 dispersions. (e) and (f) The results of the nonreciprocal light propagation for the proposed nonlinear photonic diode at λ = 532 and 671 nm, respectively. Reprinted with permission from ref. 41, Copyright 2019, Wiley-VCH. (g) Experimental results and theoretical fits for close aperture Z-scan curves of normalized transmittance and refractive index values of the GDY dispersions in different solvents. Reprinted with permission from ref. 113, Copyright 2021, Elsevier.

The high NLO refractive index has great application potential in optical devices based on the Kerr effect. Recently, the third-order NLO response of GDY was systematically studied in alcohol solvents *via* a femtosecond Z-scan technique. The experimental results showed that the NLO refractive index of GDY is about 10^{-8} cm^2 W^{-1}, which is about an order of magnitude higher than traditional two-dimensional materials.[113] In this experiment, GDY was fully dispersed in 1-propanol, and the normalized transmittance showed a typical peak and valley curve (Z = 0), implying the outstanding self-defocusing effect of GDY. As is known, the NLO refraction of the material is related to the viscosity, polarity and other physical properties of the solvent,[114,115] so a comparative test concerning different alcohol solvents was conducted (Fig. 9g). GDY is a direct narrow gap semiconductor whose refractive index depends largely on the generation of electron–hole pairs and the corresponding carrier density, and the lifetime of electron–hole pairs strongly affects the NLO response. GDY also has a wider delocalized π-electron framework than graphene, so it may also cause a more pronounced NLO refraction. In short, as a new two-dimensional semiconductor material, GDY has demonstrated promising application prospects in the field of NLO.

Nonlinear absorption behavior is an important NLO process that occurs under high-power laser excitation. The authors investigated the results of Z-scans with increasing excitation intensity at four different wavelengths at 290, 410, 532, and 1064 nm.[116] For the wavelength of 290 nm, when the excitation energy and energy density are relatively low, the normalized transmittance always maintains the same level, and it does not exhibit a nonlinear absorption behavior. When the energy density reaches the threshold of nonlinear absorption, GDY exhibits a two-photon absorption behavior. At the maximum energy density (Z = 0), a trough appears. As the excitation intensity increases, the trough gradually deepens. The other three wavelengths all show similar absorption behaviors (Fig. 10a). When the scanning ranges from ultraviolet to near-infrared, one can see that GDY exhibits low excitation intensity and large modulation depth in the ultraviolet band. The physical absorption mechanism of the whole process can be understood as that when the excitation energy density reaches the threshold of optical limiting (OL), two photons are continuously absorbed by one electron, and the excited electron is excited to a high energy level. Due to strong absorption, the transmittance will drop rapidly. From this work, it was found that compared with the infrared band, GDY has a lower threshold and a larger 2PA coefficient in the ultraviolet band. GDY has a lower Fermi level and a higher coefficient in the ultraviolet band. Compared with the infrared band during light absorption, the large energy band volume requires more electrons to fill the ultraviolet band. At this time, the optical limiting characteristic of the ultraviolet band appears. The large absorption cross-section of GDY nanosheets in the ultraviolet band highlights its advantages as an OL material, and has application prospects in the field of protective optical components and even the entire field of nonlinear absorption materials.

The broadband saturated absorption and transient absorption characteristics of GDY have been studied and proved from visible light to infrared.[117] Varying from the traditional materials such as graphene,[118] BP[119] and BP quantum dots (BPQDS),[120] GeP,[121] MoS_2,[122] MXene,[123] metal–organic frameworks (MOF),[84] and Te (Table 1),[124] GDY has a stronger nonlinear absorption, lower saturation intensity and ultrafast relaxation time. GDY is thus a promising broad-spectrum saturable absorber, which is applicable as a mode-locked element to generate ultrashort laser pulses in a laser cavity. Zhao *et al.* reported a mode-locked erbium-doped fiber laser based on a GDY saturable absorber at the wavelength of 1564.70 nm.[125] Recently, the saturated absorption properties of GDY were further researched. The wavelength dependence of the saturable absorption properties of GDY was determined at different wavelengths of laser excitation at 475, 1060, 1550, and 1800 nm.[117] GDY exhibited strong saturable absorption properties from the visible to the infrared band and it was calculated that GDY had significant β values (>1 cm GW^{-1}) (Fig. 10b). This means that GDY is well suited for a passive mode-locker to generate ultrashort laser pulses. The saturated absorption mechanism of GDY is shown in Fig. 10c. When the energy of incident light is close to the bandgap value, electrons will transfer from the valence band to the conduction band, and then the carriers (electrons and holes) generated from the light will redistribute due to cooling to form the Fermi–Dirac distribution, and phonon scattering will finally cause the carriers to return to the equilibrium state. However, if the light intensity is large enough, the photogenerated carriers will immediately occupy these energy states, and according to the Pauli blocking principle, photons can pass through GDY transparently, then GDY reaches saturation. In this work, high power mode-locked pulse outputs at 1 μm and 1.5 μm have been achieved by applying GDY as a saturable absorber to a fiber laser. A highly stable continuous-wave mode-locked laser pulse train was obtained (Fig. 11a). The above output performance suggests the fine output performance of the laser. GDY plays a critical role in the manufacture of ultrafast photonic devices in the communication band. Recently, the application of GDY was explored in mid-infrared ultrafast photonics.[126] Experimental results clarify that its nonlinear parameters are better than the existing mainstream two-dimensional materials. Using GDY as a saturable absorber, stable mode-locked and chaotic pulses were obtained at 1.5 μm (Fig. 11b). Also, as a mode-locked device for thulium-doped fiber lasers, high-power pulse output was obtained in the 2 μm band (Fig. 11c). The maximum output power of this laser is as high as 36.4 mW, which is better than graphene (1.21 mW).[127–130] The natural chemical and physical structure of GDY endows it with extraordinary responsiveness in the employment of nonlinear absorption. The development of new graphdiyne-based materials for the exploration of NLO is a hot topic in current scientific research. Recently, Wong *et al.* prepared two independent mercurialised graphyne nanosheets through an interface-assisted bottom-up approach.[131] In this work, the authors incorporated metallic elements as a new molecular functional form into the framework of graphdiynes to obtain metallic graphynes. The nanosheets exhibited a layered molecular structure arrangement, controlled thickness and enhanced π-conjugation, which, in turn, combined the advantages of metal centres and GDY, resulting in stable and excellent broadband nonlinear saturable absorption properties at

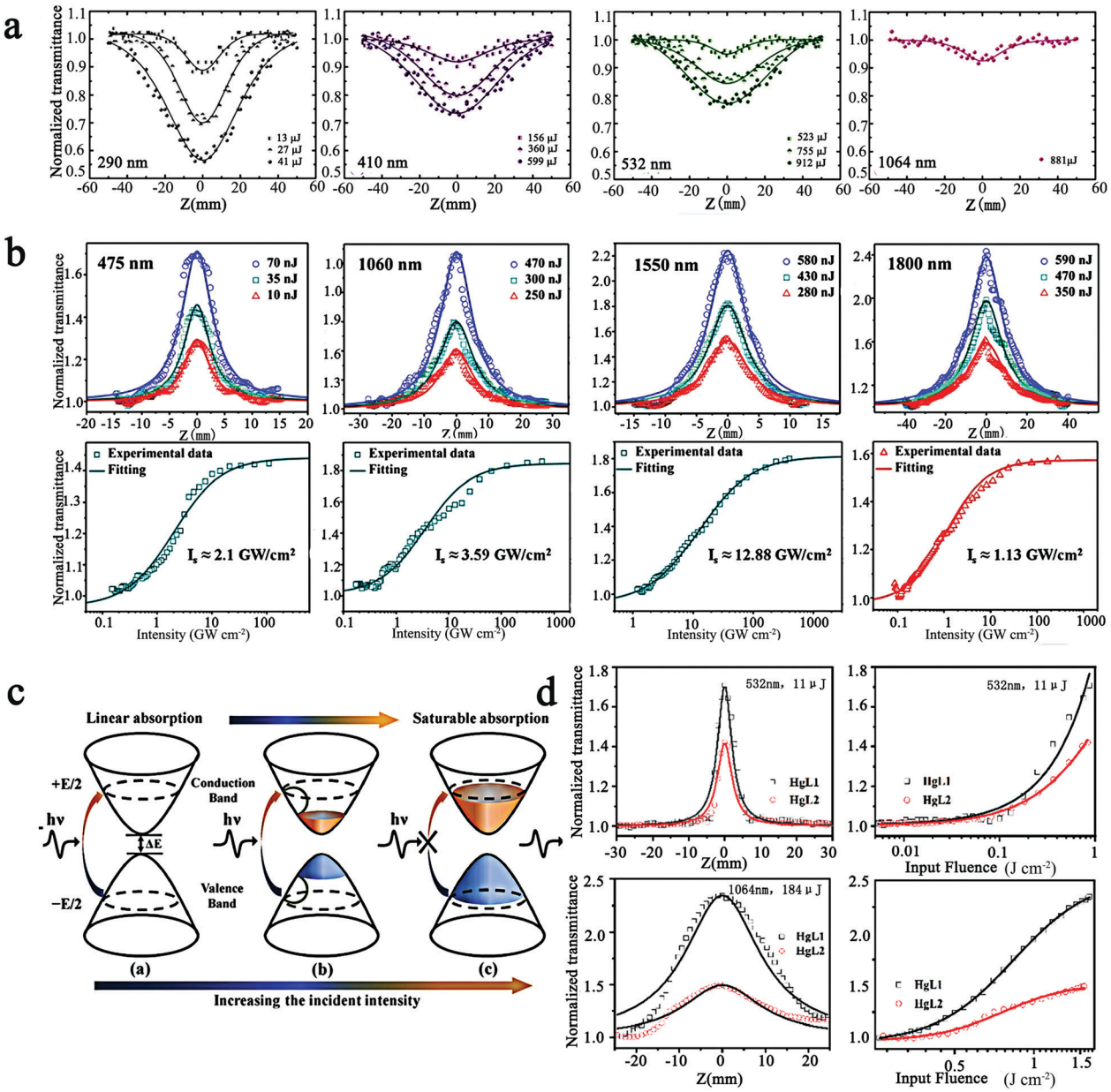

Fig. 10 (a) NLA results in the ns open-aperture Z-scan set-up of GDY nanosheets with the four excitation wavelengths. Reprinted with permission from ref. 116, Copyright 2020, The Royal Society of Chemistry. (b) Open aperture Z-scan measurements of the GDY nanocomposite at 475 nm, 1060 nm, 1550 nm, and 1800 nm. The relationship between the normalized transmittance of the GDY nanocomposite and input peak intensity of the femtosecond laser at 475 nm, 1060 nm, 1550 nm, and 1800 nm. (c) Mechanism of the GDY nanocomposite saturated absorption. Reprinted with permission from ref. 117, Copyright 2020, Wiley-VCH. (d) NLO properties of graphyne organometallic nanosheets (MGONS). Reprinted with permission from ref. 131, Copyright 2021, Wiley-VCH.

532 nm and 1064 nm (Fig. 10d). The periodic molecular framework of Hg(II)–polyynes leads to a Pauli blocking effect, causing the saturable absorption behaviour of this nanosheet, and the NLO effect is enhanced by the copolymerisation of organic polyynes with Hg(II) ions.[132,133] Subsequently, the nanosheet was used as a saturable absorber in a passively Q-switched laser, and stable pulse output characteristics were obtained (Fig. 11d and e). This shows that metallized graphdiynes materials have unique properties and application prospects. By changing the molecular structure (such as metal chromophores, nanostructures and

Table 1 β and I_s values of various 2D materials

Materials	Laser parameters	β [cm GW^{-1}]	I_s [GW cm^{-2}]	Ref.
Graphene	800 nm, 100 fs	$-(1.52 \pm 0.42) \times 10^{-2}$	583 ± 127	118
BP	800 nm, 100 fs	$-(6.17 \pm 0.19) \times 10^{-3}$	334.6 ± 43	119
BPQDS	800 nm, 100 fs	$-(0.41 \pm 0.06) \times 10^{-3}$	21.41 ± 1.87	120
GeP	800 nm, 100 fs	-4.74×10^{-1}	76.48	121
MoS_2	800 nm, 100 fs	$-(4.60 \pm 0.27) \times 10^{-3}$	413 ± 24	122
MXene	800 nm, 100 fs	−0.297	88.6 ± 5	123
MOF	800 nm, 100 fs	-3×10^{-2}	30	84
Te	800 nm, 100 fs	—	261 ± 176	124
GDY	800 nm, 100 fs	−10.96	1.89	117

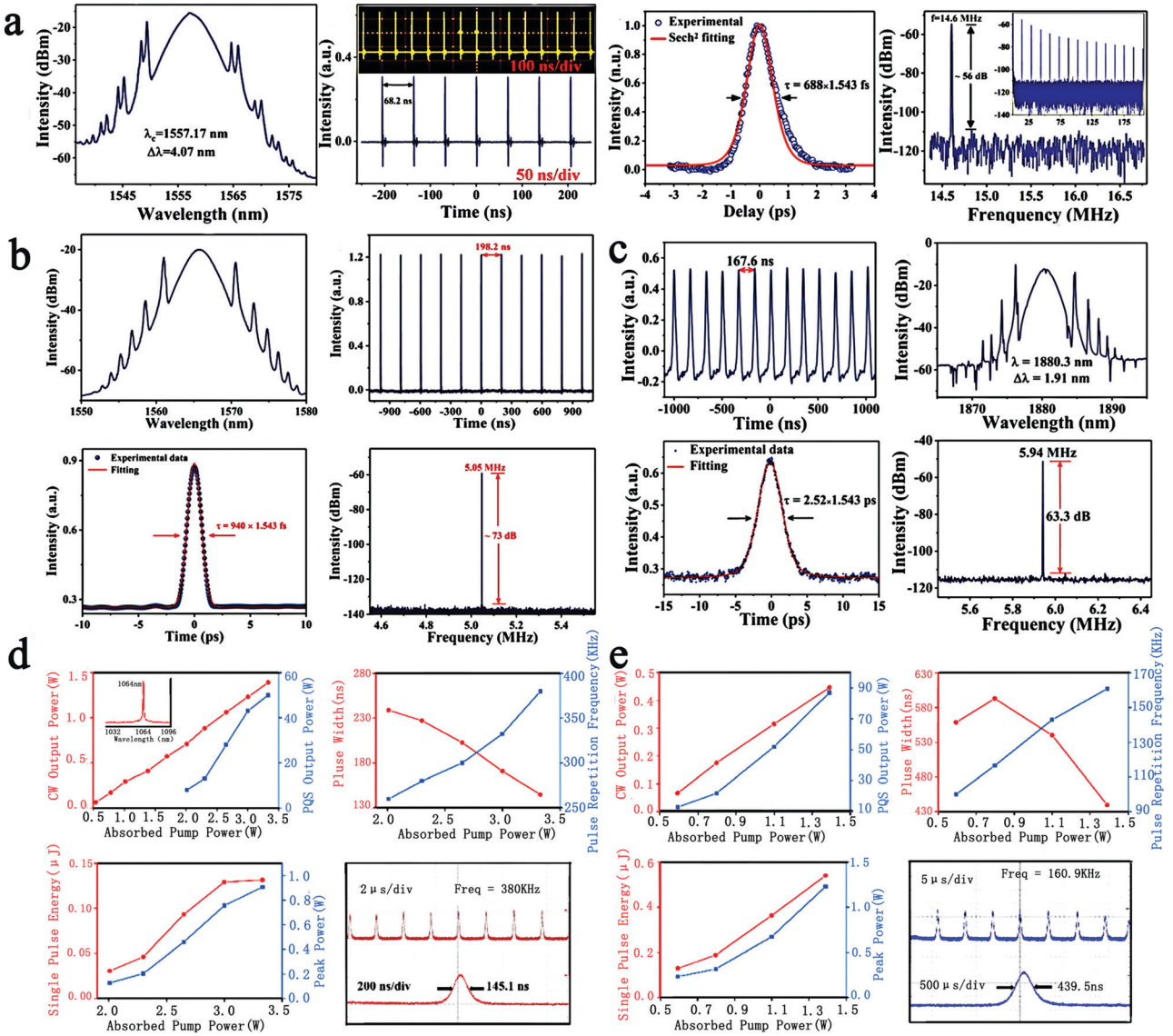

Fig. 11 (a) Mode-locked pulse output performance of the GDY nanocomposite-based EDF laser. Reprinted with permission from ref. 117, Copyright 2020, Wiley-VCH. (b) The output characteristics of the EDF laser based on GDY SA. (c) The output characteristics of the TDF laser based on GDY SA. Reprinted with permission from ref. 126, Copyright 2020, Wiley-VCH. (d) Passively Q-switched Nd:YAG laser properties with MGONS as the saturable absorber. (e) Passively Q-switched Nd:YAG laser properties with MGONS as the saturable absorber. Reprinted with permission from ref. 131, Copyright 2021, Wiley-VCH.

functional groups in ligands, *etc.*) the design of various structures of optoelectronic materials and devices is feasible.

Although GDY has been demonstrated as a promising NLO material for visible, near, and mid-infrared photonic devices, the NLO properties and applications of GDY are still under-researched. Studies on GDY are still on the rise, and future work will be devoted to the systematic study of its nonlinear properties and photonic applications.

4. Conclusion and outlook

As a new type of two-dimensional material, GDY has been extensively studied from theory to experiment for its remarkable NLO properties. The large nonlinear absorption coefficient, low saturation intensity, and ultrafast relaxation time indicate that GDY possesses outstanding potential in the field of nonlinear photonic materials. In this review, we discussed the structure, adjustable bandgap, and the linear and nonlinear optics of GDY. Nevertheless, the research on the optical properties and applications of GDY is still insufficient and there is still ample space for further exploration of optics and optoelectronics.

Scale-up and structure-controllable synthesis, and even commercialized manufacturing have always been thorny issues in the field of GDY preparations, which are crucial for the exploration of the intrinsic physical properties and the achievement of practical applications. Nevertheless, under high-temperature conditions, the coupling of the terminal alkynes of the hexaacetylenebenzene (HEB)

monomer will inevitably cause the occurrence of side reactions. The presence of oxygen atoms may also cause the oxidation of the alkynes and even the production of GDY defects. All these are obstacles that need to be overcome, and so it is a long journey to identifying and comprehensively understanding the intrinsic physical properties of the original GDY. Exploring the application of carbon–carbon triple bonds and terminal alkynes in various fields is also of great significance but the corresponding reports are still scanty at present. Therefore, the characterization and utilization of carbon–carbon triple bonds and terminal alkynes will be one of the major goals in the future. The following nonlinear characteristics and photonics applications related to GDY are worth considering in future research. First, the nonlinear characteristics benefit from the tunable bandgap of GDY, so bandgap tuning is a topic to be investigated. Modifying different superbase groups to introduce excess electrons and thus adjusting the bandgap of GDY is an effective way to enhance its NLO response. Secondly, the broadband Kerr nonlinearity and saturable absorption properties of GDY make it a promising NLO material for applications such as optical information converters, modulators and photonic diodes. Meanwhile, the introduction of chiral groups to further explore its optical properties has not yet been reported, which is an interesting and challenging topic. In addition, the introduction of large π-system molecules and electronic push–pull structures in the GDY conjugated system is highly significant for the construction of strong NLO-responsive materials.

In summary, as an emerging two-dimensional material, GDY has excellent physical and chemical properties that make it promising for various frontier applications, and GDY and its derivatives are expected to become a new generation of two-dimensional optoelectronic materials. We believe that with the progress of scientific research, GDY will shine in the field of nonlinear optics and photonics.

Conflicts of interest

There are no conflicts to declare.

Acknowledgements

Financial supports from the National Natural Science Foundation of China (21773168) and the Research Funds of Longyan University (No. LB2018016) are gratefully acknowledged.

Notes and references

1 F. Diederich and Y. Rubin, Synthetic Approaches toward Molecular and Polymeric Carbon Allotropes, *Angew. Chem., Int. Ed. Engl.*, 1992, **31**, 1101–1123.
2 H. W. Kroto, J. R. Heath, S. C. O'Brien, R. F. Curl and R. E. Smalley, C60: Buckminsterfullerene, *Nature*, 1985, **318**, 162–163.
3 J. L. Wragg, J. E. Chamberlain, H. W. White, W. Krätschmer and D. R. Huffman, Scanning tunnelling microscopy of solid C60/C70, *Nature*, 1990, **348**, 623–624.
4 J. Liu, A. G. Rinzler, H. Dai, J. H. Hafner, R. K. Bradley, P. J. Boul, A. Lu, T. Iverson, K. Shelimov, C. B. Huffman, F. Rodriguez-Macias, Y.-S. Shon, T. R. Lee, D. T. Colbert and R. E. Smalley, Fullerene Pipes, *Science*, 1998, **280**, 1253.
5 S. Iijima, Helical microtubules of graphitic carbon, *Nature*, 1991, **354**, 56–58.
6 K. S. Novoselov, A. K. Geim, S. V. Morozov, D. Jiang, Y. Zhang, S. V. Dubonos, I. V. Grigorieva and A. A. Firsov, Electric Field Effect in Atomically Thin Carbon Films, *Science*, 2004, **306**, 666.
7 X. Huang, Z. Yin, S. Wu, X. Qi, Q. He, Q. Zhang, Q. Yan, F. Boey and H. Zhang, Graphene-Based Materials: Synthesis, Characterization, Properties, and Applications, *Small*, 2011, **7**, 1876–1902.
8 F. Diederich, Carbon scaffolding: building acetylenic all-carbon and carbon-rich compounds, *Nature*, 1994, **369**, 199–207.
9 J. A. Marsden, J. J. Miller and M. M. Haley, Let the Best Ring Win: Selective Macrocycle Formation through Pd-Catalyzed or Cu-Mediated Alkyne Homocoupling, *Angew. Chem., Int. Ed.*, 2004, **43**, 1694–1697.
10 F. Diederich and M. Kivala, All-Carbon Scaffolds by Rational Design, *Adv. Mater.*, 2010, **22**, 803–812.
11 M. J. Rice, A. R. Bishop and D. K. Campbell, Unusual Soliton Properties of the Infinite Polyyne Chain, *Phys. Rev. Lett.*, 1983, **51**, 2136–2139.
12 W. A. Chalifoux and R. R. Tykwinski, Synthesis of polyynes to model the sp-carbon allotrope carbyne, *Nat. Chem.*, 2010, **2**, 967–971.
13 K. Kaiser, L. M. Scriven, F. Schulz, P. Gawel, L. Gross and H. L. Anderson, An sp-hybridized molecular carbon allotrope, cyclo[18]carbon, *Science*, 2019, **365**, 1299.
14 R. H. Baughman, H. Eckhardt and M. Kertesz, Structure–property predictions for new planar forms of carbon: Layered phases containing sp2 and sp atoms, *J. Chem. Phys.*, 1987, **87**, 6687–6699.
15 R. Sakamoto, N. Fukui, H. Maeda, R. Matsuoka, R. Toyoda and H. Nishihara, Graphdiynes: The Accelerating World of Graphdiynes (Adv. Mater. 42/2019), *Adv. Mater.*, 2019, **31**, 1970297.
16 V. R. Coluci, D. S. Galvão and R. H. Baughman, Theoretical investigation of electromechanical effects for graphyne carbon nanotubes, *J. Chem. Phys.*, 2004, **121**, 3228–3237.
17 M. M. Haley, S. C. Brand and J. J. Pak, Carbon Networks Based on Dehydrobenzoannulenes: Synthesis of Graphdiyne Substructures, *Angew. Chem., Int. Ed. Engl.*, 1997, **36**, 836–838.
18 N. Narita, S. Nagai, S. Suzuki and K. Nakao, Optimized geometries and electronic structures of graphyne and its family, *Phys. Rev. B: Condens. Matter Mater. Phys.*, 1998, **58**, 11009–11014.
19 G. Li, Y. Li, H. Liu, Y. Guo, Y. Li and D. Zhu, Architecture of graphdiyne nanoscale films, *Chem. Commun.*, 2010, **46**, 3256–3258.
20 C. Huang, Y. Li, N. Wang, Y. Xue, Z. Zuo, H. Liu and Y. Li, Progress in Research into 2D Graphdiyne-Based Materials, *Chem. Rev.*, 2018, **118**, 7744–7803.

21 J. Li, C. Wan, C. Wang, H. Zhang and X. Chen, 2D Material Chemistry: Graphdiyne-based Biochemical Sensing, *Chem. Res. Chin. Univ.*, 2020, **36**, 622–630.
22 Z. Jia, Y. Li, Z. Zuo, H. Liu, C. Huang and Y. Li, Synthesis and Properties of 2D Carbon—Graphdiyne, *Acc. Chem. Res.*, 2017, **50**, 2470–2478.
23 Y. Li, L. Xu, H. Liu and Y. Li, Graphdiyne and graphyne: from theoretical predictions to practical construction, *Chem. Soc. Rev.*, 2014, **43**, 2572–2586.
24 Y. Xue, B. Huang, Y. Yi, Y. Guo, Z. Zuo, Y. Li, Z. Jia, H. Liu and Y. Li, Anchoring zero valence single atoms of nickel and iron on graphdiyne for hydrogen evolution, *Nat. Commun.*, 2018, **9**, 1460.
25 H. Yu, Y. Xue, L. Hui, C. Zhang, Y. Li, Z. Zuo, Y. Zhao, Z. Li and Y. Li, Efficient Hydrogen Production on a 3D Flexible Heterojunction Material, *Adv. Mater.*, 2018, **30**, 1707082.
26 X. Gao, J. Li, R. Du, J. Zhou, M.-Y. Huang, R. Liu, J. Li, Z. Xie, L.-Z. Wu, Z. Liu and J. Zhang, Direct Synthesis of Graphdiyne Nanowalls on Arbitrary Substrates and Its Application for Photoelectrochemical Water Splitting Cell, *Adv. Mater.*, 2017, **29**, 1605308.
27 Y.-Y. Han, X.-L. Lu, S.-F. Tang, X.-P. Yin, Z.-W. Wei and T.-B. Lu, Metal-Free 2D/2D Heterojunction of Graphitic Carbon Nitride/Graphdiyne for Improving the Hole Mobility of Graphitic Carbon Nitride, *Adv. Energy Mater.*, 2018, **8**, 1702992.
28 W. Lan, R. Hu, D. Huang, X. Dong, G. Shen, S. Chang and D. Dai, Palladium Nanoparticles/Graphdiyne Oxide Nanocomposite with Excellent Peroxidase-like Activity and Its Application for Glutathione Detection, *Chem. Res. Chin. Univ.*, 2021, DOI: 10.1007/s40242-021-1038-1.
29 N. Wang, J. He, Z. Tu, Z. Yang, F. Zhao, X. Li, C. Huang, K. Wang, T. Jiu, Y. Yi and Y. Li, Synthesis of Chlorine-Substituted Graphdiyne and Applications for Lithium-Ion Storage, *Angew. Chem., Int. Ed.*, 2017, **56**, 10740–10745.
30 A. Bhardwaj, J. Kaur, M. Wuest and F. Wuest, In situ click chemistry generation of cyclooxygenase-2 inhibitors, *Nat. Commun.*, 2017, **8**, 1.
31 H. Du, Z. Zhang, J. He, Z. Cui, J. Chai, J. Ma, Z. Yang, C. Huang and G. Cui, A Delicately Designed Sulfide Graphdiyne Compatible Cathode for High-Performance Lithium/Magnesium–Sulfur Batteries, *Small*, 2017, **13**, 1702277.
32 J. He, N. Wang, Z. Cui, H. Du, L. Fu, C. Huang, Z. Yang, X. Shen, Y. Yi, Z. Tu and Y. Li, Hydrogen substituted graphdiyne as carbon-rich flexible electrode for lithium and sodium ion batteries, *Nat. Commun.*, 2017, **8**, 1172.
33 P. Simon and Y. Gogotsi, Materials for electrochemical capacitors, *Nat. Mater.*, 2008, **7**, 845–854.
34 M. S. Whittingham, Lithium Batteries and Cathode Materials, *Chem. Rev.*, 2004, **104**, 4271–4302.
35 N. Parvin, Q. Jin, Y. Wei, R. Yu, B. Zheng, L. Huang, Y. Zhang, L. Wang, H. Zhang, M. Gao, H. Zhao, W. Hu, Y. Li and D. Wang, Few-Layer Graphdiyne Nanosheets Applied for Multiplexed Real-Time DNA Detection, *Adv. Mater.*, 2017, **29**, 1606755.
36 Z. Xue, M. Zhu, Y. Dong, T. Feng, Z. Chen, Y. Feng, Z. Shan, J. Xu and S. Meng, An integrated targeting drug delivery system based on the hybridization of graphdiyne and MOFs for visualized cancer therapy, *Nanoscale*, 2019, **11**, 11709–11718.
37 H. Wei, R. Shi, L. Sun, H. Yu, J. Gong, C. Liu, Z. Xu, Y. Ni, J. Xu and W. Xu, Mimicking efferent nerves using a graphdiyne-based artificial synapse with multiple ion diffusion dynamics, *Nat. Commun.*, 2021, **12**, 1068.
38 Z. Jin, M. Yuan, H. Li, H. Yang, Q. Zhou, H. Liu, X. Lan, M. Liu, J. Wang, E. H. Sargent and Y. Li, Graphdiyne: An Efficient Hole Transporter for Stable High-Performance Colloidal Quantum Dot Solar Cells, *Adv. Funct. Mater.*, 2016, **26**, 5284–5289.
39 J. Xiao, J. Shi, H. Liu, Y. Xu, S. Lv, Y. Luo, D. Li, Q. Meng and Y. Li, Efficient $CH_3NH_3PbI_3$ Perovskite Solar Cells Based on Graphdiyne (GD)-Modified P3HT Hole-Transporting Material, *Adv. Energy Mater.*, 2015, **5**, 1401943.
40 H. Ren, H. Shao, L. Zhang, D. Guo, Q. Jin, R. Yu, L. Wang, Y. Li, Y. Wang, H. Zhao and D. Wang, A New Graphdiyne Nanosheet/Pt Nanoparticle-Based Counter Electrode Material with Enhanced Catalytic Activity for Dye-Sensitized Solar Cells, *Adv. Energy Mater.*, 2015, **5**, 1500296.
41 L. Wu, Y. Dong, J. Zhao, D. Ma, W. Huang, Y. Zhang, Y. Wang, X. Jiang, Y. Xiang, J. Li, Y. Feng, J. Xu and H. Zhang, Kerr Nonlinearity in 2D Graphdiyne for Passive Photonic Diodes, *Adv. Mater.*, 2019, **31**, 1807981.
42 X. Jiang, X. Zhao, W. Bao, R. Shi, J. Zhao, J. Kang, X. Xia, H. Chen, H. Li, J. Xu and H. Zhang, Graphdiyne Nanosheets for Multicolor Random Lasers, *ACS Appl. Nano Mater.*, 2020, **3**, 4990–4996.
43 F. Xia, H. Wang, D. Xiao, M. Dubey and A. Ramasubramaniam, Two-dimensional material nanophotonics, *Nat. Photonics*, 2014, **8**, 899–907.
44 X. Miao, N. Xuan, Q. Liu, W. Wu, H. Liu, Z. Sun and M. Ji, Optimizing Nonlinear Optical Visibility of Two-Dimensional Materials, *ACS Appl. Mater. Interfaces*, 2017, **9**, 34448–34455.
45 J. Zhou, J. Li, Z. Liu and J. Zhang, Exploring Approaches for the Synthesis of Few-Layered Graphdiyne, *Adv. Mater.*, 2019, **31**, 1803758.
46 H. Yu, Y. Xue and Y. Li, Graphdiyne and its Assembly Architectures: Synthesis, Functionalization, and Applications, *Adv. Mater.*, 2019, **31**, 1803101.
47 Y. Z. S. Zhan, N. Yang and D. Wang, Pore Structure of Graphdiyne: Design, Synthesis and Application, *Chem. J. Chin. Univ.*, 2020, **42**, 333–348.
48 N. Hebert, A. Beck, R. B. Lennox and G. Just, A new reagent for the removal of the 4-methoxybenzyl ether: application to the synthesis of unusual macrocyclic and bolaform phosphatidylcholines, *J. Org. Chem.*, 1992, **57**, 1777–1783.
49 X. Qian, Z. Ning, Y. Li, H. Liu, C. Ouyang, Q. Chen and Y. Li, Construction of graphdiyne nanowires with high-conductivity and mobility, *Dalton Trans.*, 2012, **41**, 730–733.
50 J. Zhou, X. Gao, R. Liu, Z. Xie, J. Yang, S. Zhang, G. Zhang, H. Liu, Y. Li, J. Zhang and Z. Liu, Synthesis of Graphdiyne Nanowalls Using Acetylenic Coupling Reaction, *J. Am. Chem. Soc.*, 2015, **137**, 7596–7599.
51 R. Matsuoka, R. Sakamoto, K. Hoshiko, S. Sasaki, H. Masunaga, K. Nagashio and H. Nishihara, Crystalline

Graphdiyne Nanosheets Produced at a Gas/Liquid or Liquid/Liquid Interface, *J. Am. Chem. Soc.*, 2017, **139**, 3145–3152.
52 F. Zhao, N. Wang, M. Zhang, A. Sápi, J. Yu, X. Li, W. Cui, Z. Yang and C. Huang, In situ growth of graphdiyne on arbitrary substrates with a controlled-release method, *Chem. Commun.*, 2018, **54**, 6004–6007.
53 Z. Zuo, H. Shang, Y. Chen, J. Li, H. Liu, Y. Li and Y. Li, A facile approach for graphdiyne preparation under atmosphere for an advanced battery anode, *Chem. Commun.*, 2017, **53**, 8074–8077.
54 J. Li, J. Xu, Z. Xie, X. Gao, J. Zhou, Y. Xiong, C. Chen, J. Zhang and Z. Liu, Diatomite-Templated Synthesis of Freestanding 3D Graphdiyne for Energy Storage and Catalysis Application, *Adv. Mater.*, 2018, **30**, 1800548.
55 J. Li, Y. Xiong, Z. Xie, X. Gao, J. Zhou, C. Yin, L. Tong, C. Chen, Z. Liu and J. Zhang, Template Synthesis of an Ultrathin β-Graphdiyne-Like Film Using the Eglinton Coupling Reaction, *ACS Appl. Mater. Interfaces*, 2019, **11**, 2734–2739.
56 Q. Pan, S. Chen, C. Wu, F. Shao, J. Sun, L. Sun, Z. Zhang, Y. Man, Z. Li, L. He and Y. Zhao, Direct Synthesis of Crystalline Graphtetrayne—A New Graphyne Allotrope, *CCS Chem.*, 2021, **3**, 1368–1375.
57 J. Liu, C. Chen and Y. Zhao, Progress and Prospects of Graphdiyne-Based Materials in Biomedical Applications, *Adv. Mater.*, 2019, **31**, 1804386.
58 H. Qiu, M. Xue, C. Shen, Z. Zhang and W. Guo, Graphynes for Water Desalination and Gas Separation, *Adv. Mater.*, 2019, **31**, 1803772.
59 R. Sakamoto, N. Fukui, H. Maeda, R. Matsuoka, R. Toyoda and H. Nishihara, The Accelerating World of Graphdiynes, *Adv. Mater.*, 2019, **31**, 1804211.
60 C. N. D. Malko, F. Vines and A. Gorling, Competition for Graphene: Graphynes with Direction-Dependent Dirac Cones, *Phys. Rev. Lett.*, 2012, **108**(8), 086804.
61 H.-J. Cui, X.-L. Sheng, Q.-B. Yan, Q.-R. Zheng and G. Su, Strain-induced Dirac cone-like electronic structures and semiconductor–semimetal transition in graphdiyne, *Phys. Chem. Chem. Phys.*, 2013, **15**, 8179–8185.
62 G. Luo, X. Qian, H. Liu, R. Qin, J. Zhou, L. Li, Z. Gao, E. Wang, W.-N. Mei, J. Lu, Y. Li and S. Nagase, Quasiparticle energies and excitonic effects of the two-dimensional carbon allotrope graphdiyne: Theory and experiment, *Phys. Rev. B: Condens. Matter Mater. Phys.*, 2011, **84**, 075439.
63 Y. Jiao, A. Du, M. Hankel, Z. Zhu, V. Rudolph and S. C. Smith, Graphdiyne: a versatile nanomaterial for electronics and hydrogen purification, *Chem. Commun.*, 2011, **47**, 11843–11845.
64 M. Long, L. Tang, D. Wang, Y. Li and Z. Shuai, Electronic Structure and Carrier Mobility in Graphdiyne Sheet and Nanoribbons: Theoretical Predictions, *ACS Nano*, 2011, **5**, 2593–2600.
65 Q. Zheng, G. Luo, Q. Liu, R. Quhe, J. Zheng, K. Tang, Z. Gao, S. Nagase and J. Lu, Structural and electronic properties of bilayer and trilayer graphdiyne, *Nanoscale*, 2012, **4**, 3990–3996.
66 T. Ohta, A. Bostwick, T. Seyller, K. Horn and E. Rotenberg, Controlling the Electronic Structure of Bilayer Graphene, *Science*, 2006, **313**, 951.
67 L. D. Pan, L. Z. Zhang, B. Q. Song, S. X. Du and H. J. Gao, Graphyne- and graphdiyne-based nanoribbons: Density functional theory calculations of electronic structures, *Appl. Phys. Lett.*, 2011, **98**, 173102.
68 G. Luo, Q. Zheng, W.-N. Mei, J. Lu and S. Nagase, Structural, Electronic, and Optical Properties of Bulk Graphdiyne, *J. Phys. Chem. C*, 2013, **117**, 13072–13079.
69 Z.-Z. Lin, Q. Wei and X. Zhu, Modulating the electronic properties of graphdiyne nanoribbons, *Carbon*, 2014, **66**, 504–510.
70 N. Ketabi, T. M. Tolhurst, B. Leedahl, H. Liu, Y. Li and A. Moewes, How functional groups change the electronic structure of graphdiyne: Theory and experiment, *Carbon*, 2017, **123**, 1–6.
71 A. Mohajeri and A. Shahsavar, Li-decoration on the edge oxidized graphyne and graphdiyne: A first principles study, *Comput. Mater. Sci.*, 2016, **115**, 51–59.
72 B. Mortazavi, M. Shahrokhi, M. E. Madjet, T. Hussain, X. Zhuang and T. Rabczuk, N-, B-, P-, Al-, As-, and Ga-graphdiyne/graphyne lattices: first-principles investigation of mechanical, optical and electronic properties, *J. Mater. Chem. C*, 2019, **7**, 3025–3036.
73 X. Li and S. Li, Investigations of electronic and nonlinear optical properties of single alkali metal adsorbed graphene, graphyne and graphdiyne systems by first-principles calculations, *J. Mater. Chem. C*, 2019, **7**, 1630–1640.
74 Y. Moriya, T. Takata and K. Domen, Recent progress in the development of (oxy)nitride photocatalysts for water splitting under visible-light irradiation, *Coord. Chem. Rev.*, 2013, **257**, 1957–1969.
75 T. Le Bahers, M. Rérat and P. Sautet, Semiconductors Used in Photovoltaic and Photocatalytic Devices: Assessing Fundamental Properties from DFT, *J. Phys. Chem. C*, 2014, **118**, 5997–6008.
76 S. Chopra, Graphyne and graphdiyne: theoretical insight into ground and excited state properties, *RSC Adv.*, 2016, **6**, 89934–89939.
77 Z. Feng, Y. Li, Y. Tang, W. Chen, R. Li, Y. Ma and X. Dai, Two-dimensional halogen-substituted graphdiyne: first-principles investigation of mechanical, electronic, optical, and photocatalytic properties, *J. Mater. Sci.*, 2020, **55**, 8220–8230.
78 A. Mohajeri and A. Shahsavar, Tailoring the optoelectronic properties of graphyne and graphdiyne: nitrogen/sulfur dual doping versus oxygen containing functional groups, *J. Mater. Sci.*, 2017, **52**, 5366–5379.
79 S.-P. Guo, Y. Chi and G.-C. Guo, Recent achievements on middle and far-infrared second-order nonlinear optical materials, *Coord. Chem. Rev.*, 2017, **335**, 44–57.
80 T. T. Tran, H. Yu, J. M. Rondinelli, K. R. Poeppelmeier and P. S. Halasyamani, Deep Ultraviolet Nonlinear Optical Materials, *Chem. Mater.*, 2016, **28**, 5238–5258.
81 P. A. Franken, A. E. Hill, C. W. Peters and G. Weinreich, Generation of Optical Harmonics, *Phys. Rev. Lett.*, 1961, **7**, 118–119.

82 S. Lu, Y. Ge, Z. Sun, Z. Huang, R. Cao, C. Zhao, S. Wen, D. Fan, J. Li and H. Zhang, Ultrafast nonlinear absorption and nonlinear refraction in few-layer oxidized black phosphorus, *Photonics Res.*, 2016, **4**, 286–292.
83 B. J. Eggleton, B. Luther-Davies and K. Richardson, Chalcogenide photonics, *Nat. Photonics*, 2011, **5**, 141–148.
84 X. Jiang, L. Zhang, S. Liu, Y. Zhang, Z. He, W. Li, F. Zhang, Y. Shi, W. Lü, Y. Li, Q. Wen, J. Li, J. Feng, S. Ruan, Y.-J. Zeng, X. Zhu, Y. Lu and H. Zhang, Ultrathin Metal–Organic Framework: An Emerging Broadband Nonlinear Optical Material for Ultrafast Photonics, *Adv. Opt. Mater.*, 2018, **6**, 1800561.
85 Z. Sun, A. Martinez and F. Wang, Optical modulators with 2D layered materials, *Nat. Photonics*, 2016, **10**, 227–238.
86 Y. Zhao, H. Tang, N. Yang and D. Wang, 5th Anniversary Article: Graphdiyne: Recent Achievements in Photo- and Electrochemical Conversion (Adv. Sci. 12/2018), *Adv. Sci.*, 2018, **5**, 1870076.
87 Y. Dong, Y. Zhang, X. Li, Y. Feng, H. Zhang and J. Xu, Chiral Perovskites: Promising Materials toward Next-Generation Optoelectronics, *Small*, 2019, **15**, 1902237.
88 J. Xu, X. Li, J. Xiong, C. Yuan, S. Semin, T. Rasing and X.-H. Bu, Nonlinear Optical Perovskites: Halide Perovskites for Nonlinear Optics (Adv. Mater. 3/2020), *Adv. Mater.*, 2020, **32**, 2070017.
89 J. Xu, S. Semin, T. Rasing and A. E. Rowan, Organized Chromophoric Assemblies for Nonlinear Optical Materials: Towards (Sub)wavelength Scale Architectures, *Small*, 2015, **11**, 1113–1129.
90 K. M. Ok, Toward the Rational Design of Novel Noncentrosymmetric Materials: Factors Influencing the Framework Structures, *Acc. Chem. Res.*, 2016, **49**, 2774–2785.
91 C. Yuan, X. Li, S. Semin, Y. Feng, T. Rasing and J. Xu, Chiral Lead Halide Perovskite Nanowires for Second-Order Nonlinear Optics, *Nano Lett.*, 2018, **18**, 5411–5417.
92 X. Li, Graphdiyne: A promising nonlinear optical material modulated by tetrahedral alkali-metal nitrides, *J. Mol. Liq.*, 2019, **277**, 641–645.
93 Y. Bai, Z.-J. Zhou, J.-J. Wang, Y. Li, D. Wu, W. Chen, Z.-R. Li and C.-C. Sun, New Acceptor–Bridge–Donor Strategy for Enhancing NLO Response with Long-Range Excess Electron Transfer from the $NH_2\cdots M/M_3O$ Donor (M = Li, Na, K) to Inside the Electron Hole Cage $C_{20}F_{19}$ Acceptor through the Unusual σ Chain Bridge $(CH_2)_4$, *J. Phys. Chem. A*, 2013, **117**, 2835–2843.
94 A. Omidvar, Design of a Novel Series of Donor–Acceptor Frameworks via Superalkali–Superhalogen Assemblage to Improve the Nonlinear Optical Responses, *Inorg. Chem.*, 2018, **57**, 9335–9347.
95 R.-L. Zhong, H.-L. Xu, Z.-R. Li and Z.-M. Su, Role of Excess Electrons in Nonlinear Optical Response, *J. Phys. Chem. Lett.*, 2015, **6**, 612–619.
96 T.-M. Yuan, S.-L. Liu, Z.-B. Liu, X. Wang, W.-Z. Li, J.-B. Cheng and Q.-Z. Li, Nonlinear optical properties of aluminum nitride nanotubes doped by excess electron: a first principle study, *J. Mol. Model.*, 2018, **24**, 205.
97 Y.-D. Song, L. Wang and L.-M. Wu, How the alkali metal atoms affect electronic structure and the nonlinear optical properties of $C_{24}N_{24}$ nanocage, *Optik*, 2017, **135**, 139–152.
98 M. Niu, G. Yu, G. Yang, W. Chen, X. Zhao and X. Huang, Doping the Alkali Atom: An Effective Strategy to Improve the Electronic and Nonlinear Optical Properties of the Inorganic $Al_{12}N_{12}$ Nanocage, *Inorg. Chem.*, 2014, **53**, 349–358.
99 E. Shakerzadeh, Z. Biglari and E. Tahmasebi, M@B40 (M = Li, Na, K) serving as a potential promising novel NLO nanomaterial, *Chem. Phys. Lett.*, 2016, **654**, 76–80.
100 K. Shehzadi, K. Ayub and T. Mahmood, Theoretical study on design of novel superalkalis doped graphdiyne: A new donor–acceptor (D–π–A) strategy for enhancing NLO response, *Appl. Surf. Sci.*, 2019, **492**, 255–263.
101 J. Maria, R. Iqbal, R. Ludwig and K. Ayub, Phosphides or nitrides for better NLO properties? A detailed comparative study of alkali metal doped nano-cages, *Mater. Res. Bull.*, 2017, **92**, 113–122.
102 F. Ullah, N. Kosar, K. Ayub, M. A. Gilani and T. Mahmood, Theoretical study on a boron phosphide nanocage doped with superalkalis: novel electrides having significant nonlinear optical response, *New J. Chem.*, 2019, **43**, 5727–5736.
103 N. Kosar, K. Shehzadi, K. Ayub and T. Mahmood, Nonlinear optical response of sodium based superalkalis decorated graphdiyne surface: A DFT study, *Optik*, 2020, **218**, 165033.
104 N. Kosar, K. Shehzadi, K. Ayub and T. Mahmood, Theoretical study on novel superalkali doped graphdiyne complexes: Unique approach for the enhancement of electronic and nonlinear optical response, *J. Mol. Graphics Modell.*, 2020, **97**, 107573.
105 J. J. Dean and H. M. van Driel, Second harmonic generation from graphene and graphitic films, *Appl. Phys. Lett.*, 2009, **95**, 261910.
106 Y. Li, Y. Rao, K. F. Mak, Y. You, S. Wang, C. R. Dean and T. F. Heinz, Probing Symmetry Properties of Few-Layer MoS_2 and h-BN by Optical Second-Harmonic Generation, *Nano Lett.*, 2013, **13**, 3329–3333.
107 H. M. Su, J. T. Ye, Z. K. Tang and K. S. Wong, Resonant second-harmonic generation in monosized and aligned single-walled carbon nanotubes, *Phys. Rev. B: Condens. Matter Mater. Phys.*, 2008, **77**, 125428.
108 L. M. Malard, T. V. Alencar, A. P. M. Barboza, K. F. Mak and A. M. de Paula, Observation of intense second harmonic generation from MoS_2 atomic crystals, *Phys. Rev. B: Condens. Matter Mater. Phys.*, 2013, **87**, 201401.
109 D. H. Kim and D. Lim, Optical second-harmonic generation in few-layer $MoSe_2$, *J. Korean Phys. Soc.*, 2015, **66**, 816–820.
110 J. Yu, X. Kuang, J. Li, J. Zhong, C. Zeng, L. Cao, Z. Liu, Z. Zeng, Z. Luo, T. He, A. Pan and Y. Liu, Giant nonlinear optical activity in two-dimensional palladium diselenide, *Nat. Commun.*, 2021, **12**, 1083.
111 A. S. Haynes, F. O. Saouma, C. O. Otieno, D. J. Clark, D. P. Shoemaker, J. I. Jang and M. G. Kanatzidis, Phase-Change Behavior and Nonlinear Optical Second and Third Harmonic Generation of the One-Dimensional $K_{(1-x)}Cs_xPSe_6$ and Metastable β-$CsPSe_6$, *Chem. Mater.*, 2015, **27**, 1837–1846.

112 S. Deckers, J. Steverlynck, P. Willot, S. Vandendriessche, G. Koeckelberghs, I. Asselberghs, T. Verbiest and M. A. van der Veen, Regioregularity Increases Second-Order Nonlinear Optical Response of Polythiophenes in Solution, *J. Phys. Chem. C*, 2015, **119**, 18513–18517.

113 Y. Dong, S. Semin, Y. Feng, J. Xu and T. Rasing, Solvent induced enhancement of nonlinear optical response of graphdiyne, *Chin. Chem. Lett.*, 2021, **32**, 525–528.

114 B. Zhao, B. Cao, W. Zhou, D. Li and W. Zhao, Nonlinear Optical Transmission of Nanographene and Its Composites, *J. Phys. Chem. C*, 2010, **114**, 12517–12523.

115 J. E. Riggs and Y.-P. Sun, Optical Limiting Properties of [60]Fullerene and Methano[60]fullerene Derivative in Solution versus in Polymer Matrix: The Role of Bimolecular Processes and a Consistent Nonlinear Absorption Mechanism, *J. Phys. Chem. A*, 1999, **103**, 485–495.

116 F. Zhang, G. Liu, J. Yuan, Z. Wang, T. Tang, S. Fu, H. Zhang, Z. Man, F. Xing and X. Xu, 2D graphdiyne: an excellent ultraviolet nonlinear absorption material, *Nanoscale*, 2020, **12**, 6243–6249.

117 J. Guo, R. Shi, R. Wang, Y. Wang, F. Zhang, C. Wang, H. Chen, C. Ma, Z. Wang, Y. Ge, Y. Song, Z. Luo, D. Fan, X. Jiang, J. Xu and H. Zhang, Graphdiyne-Polymer Nanocomposite as a Broadband and Robust Saturable Absorber for Ultrafast Photonics, *Laser Photonics Rev.*, 2020, **14**, 1900367.

118 K. Wang, Y. Feng, C. Chang, J. Zhan, C. Wang, Q. Zhao, J. N. Coleman, L. Zhang, W. J. Blau and J. Wang, Broadband ultrafast nonlinear absorption and nonlinear refraction of layered molybdenum dichalcogenide semiconductors, *Nanoscale*, 2014, **6**, 10530–10535.

119 S. B. Lu, L. L. Miao, Z. N. Guo, X. Qi, C. J. Zhao, H. Zhang, S. C. Wen, D. Y. Tang and D. Y. Fan, Broadband nonlinear optical response in multi-layer black phosphorus: an emerging infrared and mid-infrared optical material, *Opt. Express*, 2015, **23**, 11183–11194.

120 Y. Xu, W. Wang, Y. Ge, H. Guo, X. Zhang, S. Chen, Y. Deng, Z. Lu and H. Zhang, Stabilization of Black Phosphorous Quantum Dots in PMMA Nanofiber Film and Broadband Nonlinear Optics and Ultrafast Photonics Application, *Adv. Funct. Mater.*, 2017, **27**, 1702437.

121 J. Guo, D. Huang, Y. Zhang, H. Yao, Y. Wang, F. Zhang, R. Wang, Y. Ge, Y. Song, Z. Guo, F. Yang, J. Liu, C. Xing, T. Zhai, D. Fan and H. Zhang, 2D GeP as a Novel Broadband Nonlinear Optical Material for Ultrafast Photonics, *Laser Photonics Rev.*, 2019, **13**, 1900123.

122 K. Wang, J. Wang, J. Fan, M. Lotya, A. O'Neill, D. Fox, Y. Feng, X. Zhang, B. Jiang, Q. Zhao, H. Zhang, J. N. Coleman, L. Zhang and W. J. Blau, Ultrafast Saturable Absorption of Two-Dimensional MoS_2 Nanosheets, *ACS Nano*, 2013, **7**, 9260–9267.

123 X. Jiang, S. Liu, W. Liang, S. Luo, Z. He, Y. Ge, H. Wang, R. Cao, F. Zhang, Q. Wen, J. Li, Q. Bao, D. Fan and H. Zhang, Broadband Nonlinear Photonics in Few-Layer MXene $Ti_3C_2T_x$ (T = F, O, or OH), *Laser Photonics Rev.*, 2018, **12**, 1700229.

124 K. Wang, X. Zhang, I. M. Kislyakov, N. Dong, S. Zhang, G. Wang, J. Fan, X. Zou, J. Du, Y. Leng, Q. Zhao, K. Wu, J. Chen, S. M. Baesman, K.-S. Liao, S. Maharjan, H. Zhang, L. Zhang, S. A. Curran, R. S. Oremland, W. J. Blau and J. Wang, Bacterially synthesized tellurium nanostructures for broadband ultrafast nonlinear optical applications, *Nat. Commun.*, 2019, **10**, 3985.

125 Y. Zhao, P. Guo, X. Li and Z. Jin, Ultrafast photonics application of graphdiyne in the optical communication region, *Carbon*, 2019, **149**, 336–341.

126 J. Guo, Z. Wang, R. Shi, Y. Zhang, Z. He, L. Gao, R. Wang, Y. Shu, C. Ma, Y. Ge, Y. Song, D. Fan, J. Xu and H. Zhang, Graphdiyne as a Promising Mid-Infrared Nonlinear Optical Material for Ultrafast Photonics, *Adv. Opt. Mater.*, 2020, **8**, 2000067.

127 L. M. Zhao, D. Y. Tang, H. Zhang, X. Wu, Q. Bao and K. P. Loh, Dissipative soliton operation of an ytterbium-doped fiber laser mode locked with atomic multilayer graphene, *Opt. Lett.*, 2010, **35**, 3622–3624.

128 Q. Bao, H. Zhang, Y. Wang, Z. Ni, Y. Yan, Z. X. Shen, K. P. Loh and D. Y. Tang, Atomic-Layer Graphene as a Saturable Absorber for Ultrafast Pulsed Lasers, *Adv. Funct. Mater.*, 2009, **19**, 3077–3083.

129 G. Sobon, J. Sotor, I. Pasternak, A. Krajewska, W. Strupinski and K. M. Abramski, Multilayer graphene-based saturable absorbers with scalable modulation depth for mode-locked Er- and Tm-doped fiber lasers, *Opt. Mater. Express*, 2015, **5**, 2884–2894.

130 W. Liu, Y. Zu, J. Guo, S. Huang, D. Li, J. Liu, D. Liu and Y. Ge, Watt-level graphdiyne passively Q-switched Tm:YAP laser at $\sim$2 μm, *Optik*, 2021, **242**, 167208.

131 L. Xu, J. Sun, T. Tang, H. Zhang, M. Sun, J. Zhang, J. Li, B. Huang, Z. Wang, Z. Xie and W.-Y. Wong, Metallated Graphynes as a New Class of Photofunctional 2D Organometallic Nanosheets, *Angew. Chem., Int. Ed.*, 2021, **60**, 11326–11334.

132 G.-J. Zhou, W.-Y. Wong, Z. Lin and C. Ye, White Metallopolyynes for Optical Limiting/Transparency Trade-off Optimization, *Angew. Chem., Int. Ed.*, 2006, **45**, 6189–6193.

133 G. Wang, A. A. Baker-Murray and W. J. Blau, Saturable Absorption in 2D Nanomaterials and Related Photonic Devices, *Laser Photonics Rev.*, 2019, **13**, 1800282.

